

AEROELASTIC BEHAVIOR OF COMPOSITE WINGS IN POSTBUCKLING REGIME

De Oliveira, L.C.*, Degenhardt, R.*, Klimmek, T.**
*DLR Braunschweig, **DLR Göttingen

Keywords: *Composite Wing, Aeroelasticity, Flutter, Postbuckling Design*

Abstract

The use of composite materials in aircraft manufacturing is increasing due to the advantages they offer in terms of high strength and low weight. In addition, if the composite parts are designed to work in the postbuckling regime, the weight savings and the load carrying capacity can be increased. Typical structures that can take advantage of this type of design are stringer-stiffened panels used in wings and fuselages. In the postbuckling regime, these structures show changes in the stress distribution and also reduction of stiffness due to geometric nonlinear effects. These effects may change the dynamic characteristics of the structure, such as the natural frequencies and mode shapes, which may consequently cause changes in the aeroelastic behavior of the structure. Several studies have been made to investigate the influence of geometric nonlinear effects on the flutter speed of composite panels and high-aspect ratio wings, showing that these effects can have significant influence on the flutter speed and dynamic aeroelastic response. In this paper, a study of the aeroelastic behavior of a composite wing structure designed to work in the postbuckling regime is presented. A set of flight conditions including symmetric maneuvers are considered to obtain the design loads. A sizing process is developed to set the dimensions of ribs, spars, skin panels and stringers allowing buckling on the skin panels. A finite element model is used to model the wing structure. The analysis model is generated by the parametric finite element modeling tool MODGEN. Based on a set of input parameters, an aeroelastic model composed of structural and aerodynamic models are automatically

generated. The MSC-NASTRAN solver is used to simulate the response of the structure considering the geometric nonlinearities necessary to model the behavior in the postbuckling regime, and also to calculate the steady and unsteady aerodynamic loads by the Doublet-Lattice Method.

1 Introduction

The aircraft industry is making a great effort to reduce the weight of aircraft structures applying advanced composite materials in the design. Recent design strategies have been developed to make these structures to work in the postbuckling regime, where the efficiency of the structure can be maximized, being limited only by material failure. Good examples of this type of structure are stiffened panels used in fuselages and wings. After local buckling occurs on the panels, additional loads can still be carried by the stringer-panel assembly. However, in this condition the stiffness of the structure may be reduced. The aeroelastic response of an aircraft structure is highly dependent of the stiffness distribution, therefore, when the structure is operating in the postbuckling regime, it becomes necessary to evaluate the influence of the stiffness reduction on the aeroelastic response. Recent studies about the influence of buckling and geometric nonlinear effects on the aeroelastic behavior of aircraft structures have been conducted [1]-[4]. Studies about the simulation of postbuckling on composite stiffened structures have also been conducted recently during the POSICOSS and COCOMAT projects [5]-[8]. Improvements on finite element solvers [9], development of fast

and robust analytical [13],[14] and semi-analytical [11] methods and tools for postbuckling simulation and also optimization strategies including postbuckling [12] have been subjects of recent intensive research. For preliminary design purposes, fast semi-analytical tools are the best choice, because they can provide accurate results with low computational cost. However, these tools may be limited to specific geometric configurations and loading conditions. Nonlinear finite element models may be used for complex structures providing accurate results, but with high computational cost.

In this work, two different structure designs of a composite wing will be compared. In the first design, all the structural components are constrained by material failure and buckling, which means that buckling is not allowed to occur. In the second design, buckling is allowed on the skin panels in order to decrease the weight of the wing structure. As the stiffness is also decreased for the buckling structure, it is expected that the flutter speed of the wing will change. It is also the aim of this work to investigate how much can be the reduction in the flutter speed when a postbuckling design is used.

2 Methodology

A sizing method is applied to calculate the dimensions of the structural components, using a linear static aeroelastic analysis. Minimum and maximum reserve factors for material failure and buckling are specified and used as constraints. After the convergence to a feasible solution, a nonlinear static analysis is performed to check the structural behavior accounting for geometric nonlinearities. The maximum-strain criterion is applied to the rib webs, spar segments and skin panels. In addition, the Ritz method [18] is used to calculate the elastic buckling loads of these components, which are approximated by rectangular flat plates where all the edges of the plate are considered to be simply-supported. For the skin panels, rotational springs are attached to each edge to represent the stiffness of the stringers. In this way, general boundary

conditions which vary from a simply supported edge to a clamped edge may be represented. Each plate is modeled as an anisotropic symmetric laminate and is subjected to combined bi-axial compression loads N_{xx} and N_{yy} and shear load N_{xy} . Fig. 1 shows a schematic view of the stiffened panel.

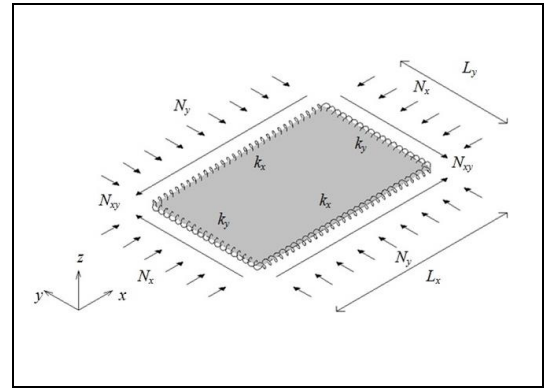


Fig. 1. Scheme for the composite panel

The Classical Laminated Plate Theory [18] is used to describe the composite material. The constitutive equation, which relates the in-plane stress resultants N and moments M with the in-plane strains ε and curvatures κ is:

$$\begin{Bmatrix} N \\ M \end{Bmatrix} = \begin{bmatrix} A & B \\ B & D \end{bmatrix} \begin{Bmatrix} \varepsilon^0 \\ \kappa \end{Bmatrix} \quad (1)$$

This work considers symmetric laminates, where the coupling stiffness matrix $[B]$ is equal to zero. The total potential energy function is calculated as a function of the transverse displacements on each plate. The displacement function w is approximated by a series of shape functions $X_i(x)$ and $Y_j(y)$ [15] which satisfy the boundary conditions on each edge of the composite plate:

$$w(x, y) = \sum_{i=1}^n \sum_{j=1}^m c_{ij} X_i(x) Y_j(y) \quad (2)$$

$$\begin{aligned} X_i(x) &= (1 - \omega_x) \sin\left(\frac{i\pi x}{L_x}\right) + \omega_x \left(\cos\left(\frac{(i-1)\pi x}{L_x}\right) - \cos\left(\frac{(i+1)\pi x}{L_x}\right) \right) \\ Y_j(y) &= (1 - \omega_y) \sin\left(\frac{j\pi y}{L_y}\right) + \omega_y \left(\cos\left(\frac{(j-1)\pi y}{L_y}\right) - \cos\left(\frac{(j+1)\pi y}{L_y}\right) \right) \end{aligned} \quad (3)$$

where c_{ij} are constants to be determined and ω_i, ω_j are calculated as a function of the rotational stiffness k_x and k_y on the edges of the plates and the stiffness constants of the laminate, in order to satisfy the boundary conditions.

The application of the Ritz method results in an eigenvalue problem dependent on the applied in-plane compressive loads N_{xx} and N_{yy} and the shear load N_{xy} :

$$[[K]-\lambda_k(N_{xx}[S_{xx}]+N_{yy}[S_{yy}]+N_{xy}[S_{xy}])]\{\Phi\}_k = \{0\} \quad (4)$$

The eigenvalues λ_k take into account the combined effect of the applied loads, and defines the actual state of the plate: if the lowest eigenvalue λ is less than 1, this indicates that plate is buckled. The eigenvectors $\{\Phi\}_k$ contain the constants values of the constants c_{ij} for each buckling mode.

3 Analysis Model

The wing model is based on an ERJ-145 aircraft [21]. Table 1 shows the geometric data of the wing and other parameters from the aircraft. The values of the cruise and diving speeds were estimated based on the aircraft data.

Description	Parameter	Unit
Wing span	20.04	(m)
Wing reference area	52.0	(m ²)
Leading Edge Sweep Angle	26.5	(degrees)
Aspect Ratio	7.7	
MTOW	22000	(kg)
MLW	19300	(kg)
MZFW	17900	(kg)
Service Ceiling	37000	(ft)
(Cruise speed)	142.0	(m/s EAS)
	0.78	Mach
(Diving speed)	164.0	(m/s EAS)
	0.89	Mach

Table 1. ERJ-145 – Wing and aircraft parameters

The aeroelastic model used to perform the analysis is composed by a finite element

model of the wing structure and an aerodynamic model. In the structural model, shell elements are used to form rib webs, spar webs and skin panels, and beam elements are used to represent stringers and also stiffeners attached to ribs and spars. The parametric model generator MODGEN [16],[17] was used to create the structural and aerodynamic models. Fig. 2 shows the layout of ribs and spars used in the structure. Fig. 3 shows a detailed view of the panels and stringers. Each skin panel is modeled by a set of shell elements in order to capture the out-of-plane displacement due to buckling. Concentrated mass elements are used to model the leading edge and trailing edge of the wing and also the fuselage and the tail. These masses are estimated based on preliminary design approaches. The mass and inertia matrix of the fuselage plus the tail is modeled by an element concentrated at the c.g. of the aircraft. Fig. 4 shows the mass elements used on the wing. Fig. 5 shows the aerodynamic model, which is composed by a set of flat panels used to represent the net pressure distribution over the wing for steady and unsteady flows. The pressure distribution is calculated by the Doublet Lattice method.

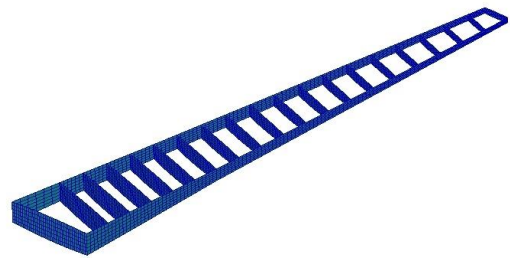


Fig. 2. Structural Layout – Ribs and Spars

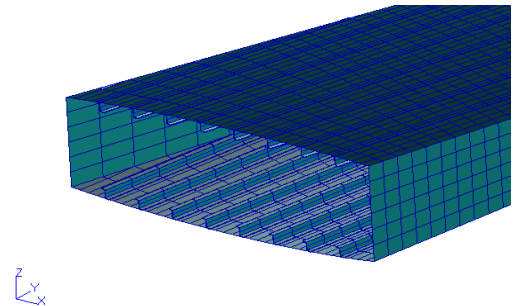


Fig. 3. Detailed view of panels and stringers

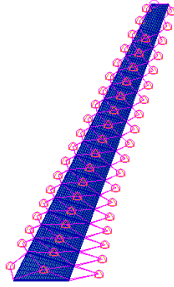


Fig. 4. Wing box and mass elements

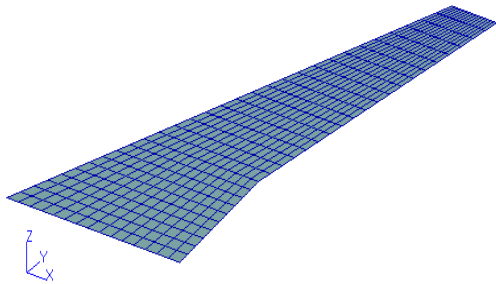


Fig. 5. Aerodynamic Model

4 Analysis Procedure

The set of parameters that are combined to form the complete set of analysis cases, which includes the aircraft c.g. position, flight altitude, speed, mass case and type of maneuver is shown on Table 2. The combination of parameters resulted in a total of 256 load cases, which were analyzed using the linear static aeroelastic solution from the MSC Nastran solver, SOL 144 [19],[20]. From the set of critical cases considering shear loads, bending moments and torsion moments, a subset of cases was selected to be used by the sizing routine, which includes the cases with higher occurrence on the envelope of the loads, as shown in Table 3.

Each iteration of the sizing process comprises the calculation of the loads for all selected critical load cases and the evaluation of the reserve factors for buckling and composite material failure. The layup of each component is fixed and the thickness is varied by the sizing process, in order to achieve a design that satisfies all the constraints for material failure and buckling. After the convergence of the

sizing process, nonlinear static analysis are performed using SOL 400 from the Nastran solver, with the critical load cases to calculate the deformed shape of the structure and evaluate the material and buckling constraints including the geometric nonlinear effects.

Parameter	Assumed Values
Speed	VC / VD
C.G. Position	Forward / Aft
Mass Cases	MTOW / MLW / MZFW / BOW
Altitudes (ft)	0 / 5000 / 10000 / 15000 / 20000 / 25000 / 30000 / 35000
Maneuvers	Pull-up 2.5g / Push-down -1.0g

Table 2. Load Case Parameters

Case	Maneuver	Speed	C.G.	Mass
1	Pull-up 2.5g	VC	Fwd	MTOW
2	Pull-up 2.5g	VD	Aft	MTOW
3	Push-down -1.0g	VC	Fwd	MTOW
4	Push-down -1.0g	VD	Aft	MTOW

Table 3. Critical Load Cases Selected for Sizing

Component	Layup
Ribs and spars	[45,-45,90,-45,90,45,90,0] _s
Panels	[0,(45,-45) ₂ ,90,0,45] _s

Table 4. Layup configuration used for each component

5 Results

The sizing process was applied to the wing structure assuming the following reserve factors: for composite material failure, minimum and maximum reserve factors of 1.8 and 2.0 were specified on both designs; for buckling, minimum and maximum reserve factors of 1.2 and 1.5 were specified on the first design, and values of 0.1 and 1.0 for the second design. Fig. 6 and Fig. 7 show a 3D view of the thickness distribution over the wing, for the non-buckling design and the postbuckling design, respectively. From Fig. 8 to Fig. 13 are shown the thickness distributions of the ribs,

spars (front and rear), upper panels and lower panels, along the span of the wing. The stringer bays are numbered from the front spar to the rear spar. It is possible to see differences in the thickness of the components, especially the skin panels. The values of the total mass obtained for the nonbuckling and buckling designs were 1130 kg and 1060 kg, respectively. This result indicates a reduction of 6% of mass of the buckling design compared to the nonbuckling design. Fig. 14 shows the deformed shape of the wing considering the design for postbuckling, obtained by a nonlinear static analysis at 90% of the limit load for the critical load case 2 (see Table 4). It is possible to see the local buckling field occurring on the upper skin, where the deformations are scaled by a factor of 2.0. Fig. 15 shows the deformed shape at 155% of the limit load, where the deformations have a factor of 1.0. It can be seen that at this point the buckling field changes from local buckling to global buckling. Fig. 16 and Fig. 17 show the results from the flutter analyses obtained for the nonbuckling design and the buckling design, respectively. The red points on the figures indicate the flutter points, where the damping factor first turns from negative to positive. Flutter speeds of 512.3 m/s and 432.3 m/s were obtained for the nonbuckling and buckling designs, respectively. This results shows a reduction of 15% in the flutter speed of the buckling design compared to the nonbuckling design.

6 Conclusions

A study of the aeroelastic behavior of a composite wing designed to work in postbuckling regime was conducted. The wing structure was sized based on a set of critical flight conditions corresponding to symmetric maneuvers. Two different designs were considered, the first being free of buckling and the second working in postbuckling under the action of the resultant loads including aerodynamic and inertia loads. The design where buckling was allowed presented a 6% reduction on the mass of the wing structure, compared to the design without buckling. The

proposed sizing process considered fixed stacking sequences for each component. Additional mass saving may be achieved if optimization of the stacking sequence on each component is conducted. The flutter speed calculated for the buckling design was 15% lower than the one for the nonbuckling design, as a result of the decrease in stiffness that follows the decrease in mass due to the smaller thicknesses obtained when the skin panels are allowed to buckle. The flutter speed for a buckling design may be increased in an optimization process where it is considered as a constraint or an objective function to be maximized. The nonlinear static analysis was conducted on the structure designed for buckling and showed that the specified buckling behavior was achieved, where the structure should present local buckling on the skin panels at the limit load. The described flutter analyses have been made considering the linear stiffness matrix of the structure. Additional studies are being conducted in order to include the geometric nonlinearities due to buckling in the calculation of the flutter speed of the composite wing.

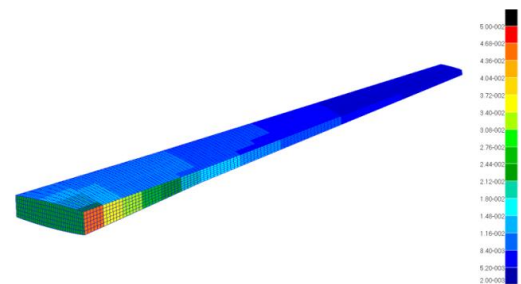


Fig. 6. Thicknesses – Nonbuckling Design

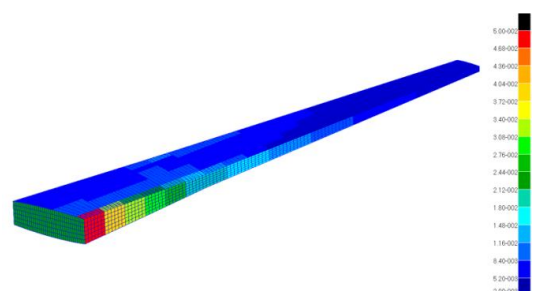


Fig. 7. Thicknesses – Buckling Design

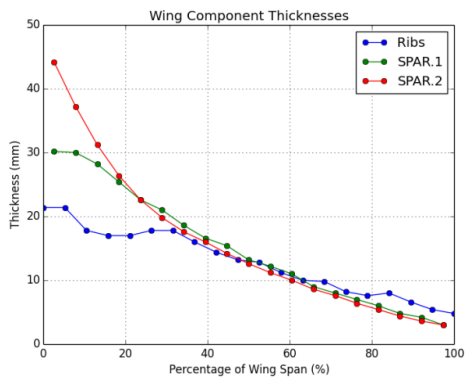


Fig. 8. Ribs and Spars – Nonbuckling design

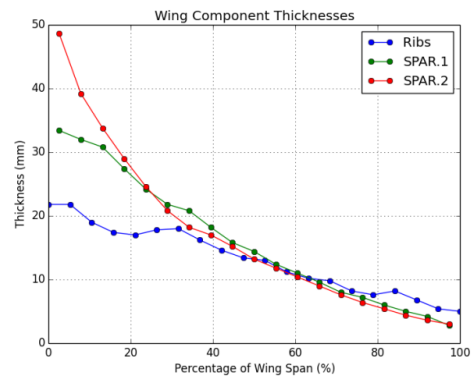


Fig. 11. Ribs and Spars – Buckling design

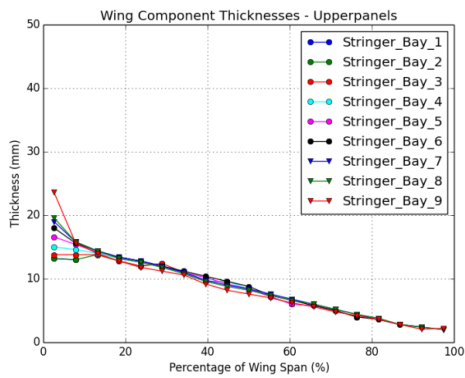


Fig. 9. Upperpanels – Nonbuckling design

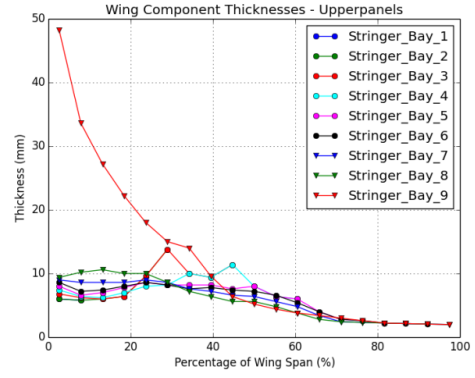


Fig. 12. Upperpanels – Buckling design

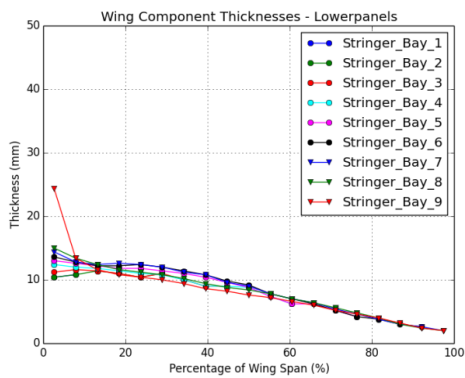


Fig. 10. Lowerpanels – Nonbuckling design

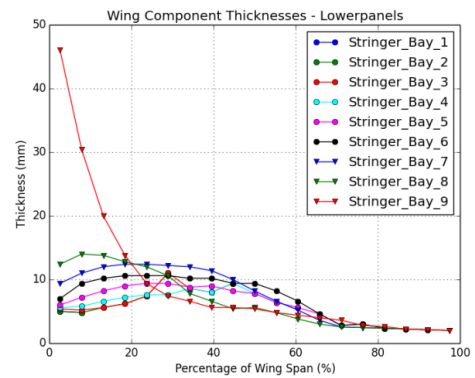


Fig. 13. Lowerpanels – Buckling design

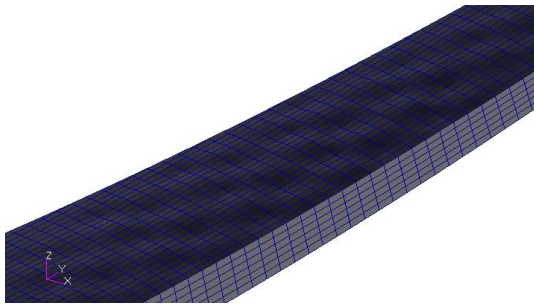


Fig. 14. Deformed shape on 90% Limit Load
Local Buckling

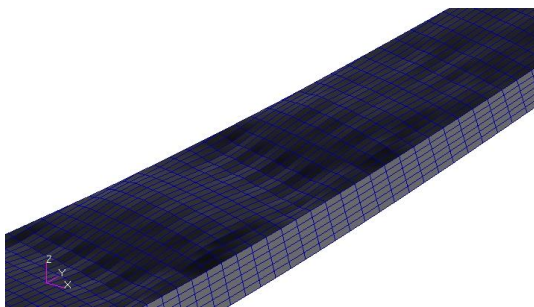


Fig. 15. Deformed shape on 155% Limit Load
Global Buckling

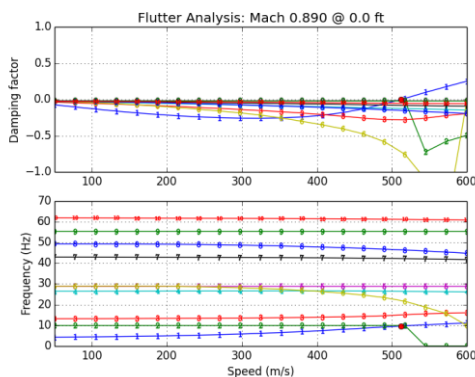


Fig. 16. Flutter Analysis – Nonbuckling Design

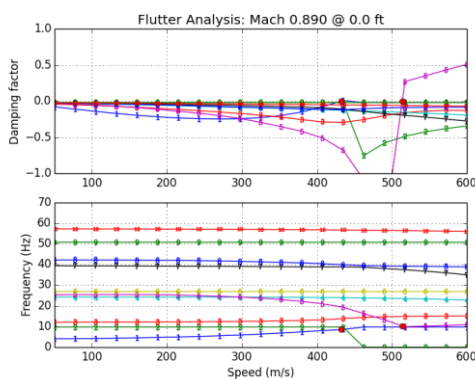


Fig. 17. Flutter Analysis – Buckling Design

References

- [1] Patil, M.J., Hodges, D.H., and Cesnik, C.E.S., "Nonlinear Aeroelasticity and Flight Dynamics of High-Altitude Long-Endurance Aircraft", *Journal of Aircraft*, Vol. 38, No. 1, 2001, pp. 88-94.
- [2] Su, W., Cesnik, C.E.S., "Nonlinear Aeroelasticity of a Very Flexible Blended-Wing-Body Aircraft", *Journal of Aircraft*, Vol. 47, No. 5, 2010, pp. 1539-1553.
- [3] Harmin, M.Y., Cooper, J.E., "Aeroelastic behavior of a wing including geometric nonlinearities", *The Aeronautical Journal*, Vol. 115, No. 1174, 2011, pp. 767-777.
- [4] Sulaeman, E., Kapania, R.K., Haftka, R.T., "Effect of Compressive Force on Flutter Speed of a Strut-Braced Wing", *AIAA Paper 2003-1943*, 44th AIAA/ASME/ASCE/AHS Structures, Structural Dynamics, and Materials Conference, 7-10 April 2003, Norfolk, Virginia.
- [5] Zimmermann, R., Rolfes, R., "POSSIC - Improved Postbuckling Simulation for Design of Fiber Composite Stiffened Fuselage Structures", *Composite Structures*, Vol. 73, 2006, pp. 171-174.
- [6] Degenhardt, R. et al., "COCOMAT - Improved Material Exploitation of Composite Airframe Structures by Accurate Simulation of Postbuckling and Collapse", *Composite Structures* No. 73, 2006, pp. 175-178.
- [7] Degenhardt, R., Kling, A., Orifici, A.C., Thomson, R.S., "Design and analysis of stiffened composite panels including post-buckling and collapse", *Computers and Structures*, No. 86, 2008, pp. 919-929.
- [8] Ghilai, G., Feldman, E., David, A., "COCOMAT - Design and Analysis Guidelines for CFRP-Stiffened Panels in Buckling and Postbuckling", *International Journal of Structural Stability and Dynamics*, Vol.10, No.4 (2010) pp 917-926.
- [9] Doreille, M., Merazzi, S., Rohwer, K., Degenhardt, R. "Post-buckling Analysis of Composite Shell Structures - Towards Fast and Accurate Tools with Implicit FEM Methods". *International Journal of Structural Stability and Dynamics*, 2009.
- [10] Orifici, A.C., Thomson, R.S., Degenhardt, R., Bisagni, C., Bayandor, J., "An Analysis Tool For Design and Certification of Postbuckling Composite Aerospace Structures", April 2009.
- [11] Bisagni, C., Vescovini, R., "Analytical formulation for local buckling and post-buckling analysis of stiffened laminated panels", *Thin-Walled Structures* 47 (2009), pp. 318-334.
- [12] Qu, S., Kennedy, D., Featherston, C.A., "A multilevel framework for optimization of an aircraft wing incorporating postbuckling effects". *Proceedings of the Institution of Mechanical Engineers, Part G: Journal of Aerospace Engineering*, published online, 9 November 2011.

- [13] Qiao, P., Shan, L., "Explicit local buckling analysis and design of fiber-reinforced plastic composite structural shapes", *Composite Structures* 70 (2005), pp. 468-483.
- [14] Mittelstedt, C., "Explicit analysis and design equations for buckling loads and minimum stiffener requirements of orthotropic and isotropic plates under compressive load braced by longitudinal stiffeners", *Thin-Walled Structures*, No. 46, 2008, pp.1409-1429.
- [15] Mittelstedt, C., "Explicit local buckling analysis of stiffened composite plates accounting for periodic boundary conditions and stiffener-plate interaction". *Composite Structures* 91 (2009), pp. 249-265.
- [16] Klimmek, T., "Parametrization of Topology and Geometry for the Multidisciplinary Optimization of Wing Structures". *Proceedings of CEAS European Air and Space Conference (CEAS2009)*, Manchester, UK, 26-29 October, 2009.
- [17] Klimmek, T., "Development of a Structural Model of the CRM Configuration for Aeroelastic and Loads Analysis". *IFASD2013 - International Forum on Aeroelasticity and Structural Dynamics 2013*, 24-26 June 2013, Bristol, UK, 2013.
- [18] Reddy, J.N. (2003), "Mechanics of Laminated Composite Plates and Shells - Theory and Analysis", CRC Press, Boca Raton, Florida, USA.
- [19] MSC/Software (2004), "MSC.Nastran Version 68 - Aeroelastic Analysis User's Guide", Santa Ana, CA, USA.
- [20] MSC/Software (2011), "MSC.Nastran 2012 - Quick Reference Guide", Santa Ana, CA, USA.
- [21] European Aviation Safety Agency (2013), "Type Certificate Data Sheet for EMB-145", No. EASA.IM.A.032, Issue 07, 08 May 2013.

Copyright Statement

The authors confirm that they, and/or their company or organization, hold copyright on all of the original material included in this paper. The authors also confirm that they have obtained permission, from the copyright holder of any third party material included in this paper, to publish it as part of their paper. The authors confirm that they give permission, or have obtained permission from the copyright holder of this paper, for the publication and distribution of this paper as part of the ICAS 2014 proceedings or as individual off-prints from the proceedings.